Numerical Investigation on the Inelastic Instability of Cruciform Columns: Effect of Material and Geometric Parameters

Meriem BelhadjAmor[1,2](✉), Mohamed Ben Bettaieb[3,4], Salah Mezlini[1], and Farid Abed-Meraim[3,4]

[1] Laboratoire de Génie Mécanique, Ecole Nationale d'Ingénieurs de Monastir, Université de Monastir, 5019 Monastir, Tunisia
mariem.belhajamor@enicar.ucar.tn

[2] Ecole Nationale d'Ingénieurs de Carthage, Université de Carthage, 2035 Tunis, Tunisia

[3] Université de Lorraine, CNRS, Arts et Métiers Institute of Technology, LEM3, 57070 Metz, France

[4] DAMAS, Laboratory of Excellence on Design of Alloy Metals for Low-mAss Structures, Université de Lorraine, Metz, France

Abstract. This work deals with a numerical investigation of the onset of inelastic instability in cruciform columns using the limit-point method. In this aim, a nonlinear buckling analysis was developed to determine the limit-point stress and the structure response during the post-buckling stage. Both total deformation and flow theories are used to describe the mechanical behavior. The numerical simulations were carried out considering cruciform columns with different material and geometric parameters. The obtained results were compared with experimental data from existing literature focused on the influence of the plasticity theory. The influences of the slenderness ratio and material parameters are discussed.

Keywords: Inelastic instability · Cruciform columns · Nonlinear FE analysis · Riks method

1 Introduction

Buckling is a common instability phenomenon in engineering applications, where the structure suddenly collapses involving very large displacements and deflections. It is well known that straight and slender thin-walled structures, such as plates and closed section columns subjected to compression loads, are likely to exhibit elastic buckling in bending mode. However, the cruciform column, which is an open thin-walled column, tends to buckle in the torsion mode according to its aspect ratio (length/section dimension) and slenderness ratio (section dimension/shell thickness) (Behzadi-Sofiani, Gardner, & Wadee, 2023). Buckling analyses of thick-walled and/or compact columns are more challenging, as plasticity may occur before buckling, referred to as plastic buckling. Research on plastic buckling dates back to 1889 with Engesser study (Engesser, 1889) that substitutes the Young modulus in the Euler buckling load formula with the tangent modulus, then with the reduced modulus, which was validated by several contributions (see, e.g., Hutchinson, 1974 and Gerard, 1962). More recently, several analytical and numerical studies have been carried out to model the plastic buckling of thin and thick-walled structures using different plasticity theories, in particular classical flow and deformation theories (Shamass, Alfano, & Guarracino, 2014). These investigations have again confirmed that the flow theory of plasticity fails to provide accurate buckling predictions. In contrast, the deformation theory shows good agreement with experimental results, albeit with weaker physical robustness than flow theory. The cruciform column is widely considered in the literature to discuss the discrepancy between the two plasticity theories (Guarracino & Simonelli, 2017). The authors of the latter reference have conducted an accurate analysis of the inelastic torsional buckling of a cruciform column by proposing numerical and analytical procedures. Their approach is based on the introduction of a small initial geometric imperfection, which is widely adopted in numerical buckling analyses (Hutchinson & Budiansky, 1976, Zhoua, et al., 2021 and Shamass, Alfano, & Guarracino, 2015).

In this work, our aim is to shed further light on the inelastic instability of cruciform columns using a nonlinear Finite Element (FE) model based on the Riks method. The buckling behavior of specimens with different slenderness ratios and various hardening parameters is then investigated using the flow and deformation plasticity theories. Numerical results are compared with experimental findings conducted by Hopperstad et al. (Hopperstad et al., 1999).

2 Finite Element Modeling

The buckling behavior of cruciform columns was numerically analyzed using Abaqus/Standard. For comparison, we consider specimens experimentally tested in the literature (Hopperstad et al., 1999). The simulated columns have a length l, a cross-section dimension b and a thickness t, as shown in Fig. 1. Table 1 presents the geometric parameters, aspect ratios, and slenderness ratios considered in the different simulations. In order to meet the kinematics of the experimental test, the end sections $z = 0$ and $z = l$ have free displacements along x and y axes, but constrained rotations ($\varphi_x = \varphi_y = \varphi_z = 0$). The cruciform column is subjected to axial compression by imposing a uniform displacement $u_z = u$ on the end section $z = l$, as shown in Fig. 1. A four-node shell element (S4) was used to mesh the specimen. The optimum element number was determined on the basis of a mesh sensitivity study.

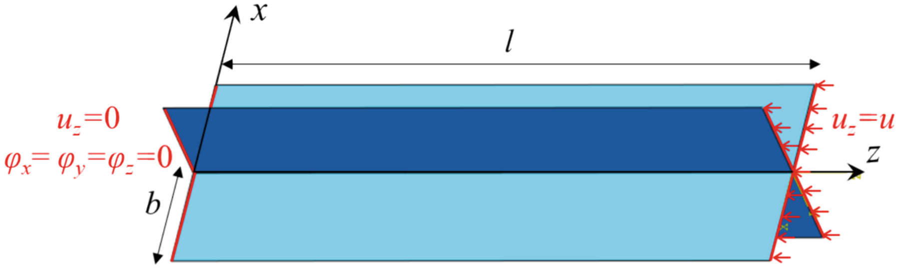

Fig. 1. Geometry and boundary conditions of the FE model.

Two series of cruciform columns (S1 and S2) were simulated to evaluate the effect of the slenderness ratio b/t. This ratio takes the values 10.5 and 30.5 to represent compact and slender columns, respectively. For each value of b/t, , two tempers of alloy AA6082 (T4 and T6) with various material parameters were examined. The Ramberg–Osgood law (Ramberg & Osgood, 1943), which is commonly used to analytically describe the nonlinear constitutive behavior of aluminum alloys, is used to model the stress-strain relationship $\sigma - \varepsilon$ (Köllnera, Gardnerb, & Wadee, 2023), thus:

$$\varepsilon = \frac{\sigma}{\mathrm{E}} + k\frac{\sigma_0}{\mathrm{E}}\left(\frac{\sigma}{\sigma_0}\right)^c, \tag{1}$$

where E is the Young modulus, σ_0 is a nominal yield stress, c and k are the hardening parameters. The used values of theses parameters are displayed in Table 1.

Table 1. Characteristics of the simulated columns.

Series	Temper	b (*mm*)	l (*mm*)	t (*mm*)	b/t	l/b	E (GPa)	σ_0 (MPa)	k	c
S1	T4	262.5	1500	25	10.5	5.714	69.7	131	1.064	23
	T6	262.5	1500	25	10.5	5.714	67.9	267	0.509	45
S2	T4	762.5	4500	25	30.5	5.902	69.7	131	1.064	23
	T6	762.5	4500	25	30.5	5.902	67.9	267	0.509	45

FE analyses were performed to detect the onset of inelastic instability for these columns. It was assumed that columns present unavoidable geometric imperfections that may influence the critical stress and the post-buckling behavior (Hutchinson & Budiansky, 1976). This analysis was carried out in two stages:

(1) In the first stage, a linear eigenvalue buckling analysis was performed using the *Buckle* Module in Abaqus/Standard, assuming linear material and geometric behavior. The results obtained from these simulations are mainly the elastic buckling stresses and eigenmodes of the columns.

(2) In the second stage, a nonlinear analysis was conducted using the Riks method, accounting for geometric and material nonlinearities and considering an initial geometric imperfection. This imperfection was introduced by scaling and adding the first buckling eigenmode, which was obtained in the initial stage, to the straight column. Our simulations were achieved with a scaling factor equal to 10% of the flange thickness (t).

3 Results and Discussion

3.1 Linear FE Analysis: Elastic Buckling

In order to validate the applied boundary conditions, the buckling mode shape was determined and compared to the deformed shape observed in the experimental test (See Fig. 2). As the simulated columns have similar aspect ratios l/b and boundary conditions, they exhibit the same buckling mode shape. It is clear that the numerically predicted buckling mode aligns with the experimental one, thus validating the modeled boundary conditions.

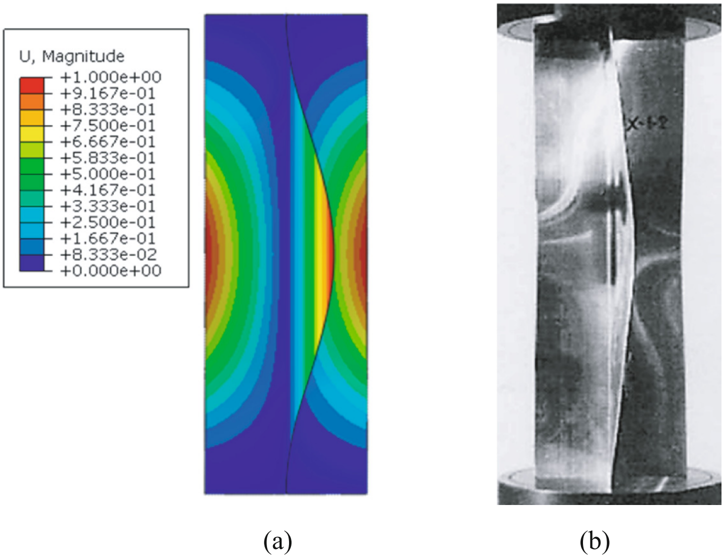

Fig. 2. First buckling mode of the column with $b/t = 30.5$ in T6 from: (a) Linear FE model (b) Experimental test.

The critical buckling stresses σ_{cr}^{LFE} evaluated by the linear FE model are compared to the theoretical predictions obtained by the Stowell theory denoted σ_{cr}^{Theo} (Gerard & Becker, 1957) as well as to the experimental measurements (σ_{cr}^{Exp}), as presented in Table 2. The relative deviation is given between parentheses. The numerical results are in good agreement with the theoretical outcomes. Regarding the experimental results, it is evident that the slender columns ($b/t = 30.5$) exhibit buckling at critical stresses, which closely correspond to the estimated elastic values, with little effect of material properties. However, for the compact columns ($b/t = 10.5$), the experimental buckling stresses are much lower than their elastic counterparts. It is worth noting here that the material behavior has a significant effect on the experimental results. Indeed, temper T4, known for its notably greater strain hardening characteristics compared to temper T6, demonstrates a more pronounced deviation from the elastic predictions. These observations substantiate the possibility of inelastic instability manifesting in the cruciform column due to variations in material and geometric parameters. We will address the inelastic buckling of these specimens in the following section.

Table 2. Comparison of elastic critical stresses and experimental results.

Series	Temper	$\sigma_{cr}^{LFE}(MPa)$	$\sigma_{cr}^{Theo}(MPa)$	$\sigma_{cr}^{Exp}(MPa)$
S1	T4	298.39	309.15 **(3.5%)**	124 **(82.6%)**
	T6	290.57	301.16 **(3.6%)**	218 **(28.5%)**
S2	T4	35.59	36.11 **(1.5%)**	40 **(11.7%)**
	T6	34.66	35.18 **(1.5%)**	38 **(9.2%)**

3.2 Nonlinear FE Analysis: Inelastic Buckling

In order to evaluate the inelastic buckling behavior of cruciform columns, nonlinear analysis was conducted using both theories of plasticity, namely, the flow theory and the deformation theory. As the Riks method is a limit-point method, the instability behavior can be investigated by evaluating the limit-point buckling (i.e. the maximum load) in the stress-displacement curves presented in Fig. 3 and 4. Hopperstad et al. (Hopperstad et al., 1999) determined the bifurcation critical stress σ_{cr}^{Exp}, which is defined as the stress level at which lateral deflections were visually observed during testing, as well as the ultimate strength σ_{u}^{Exp}. The ultimate strength is the maximum stress that a column can reach prior to the drop of its load-carrying capacity. To achieve a realistic and accurate comparison, the limit-point stress should be compared with the ultimate strength of the structure. Numerical results obtained with the flow and the deformation theories were compared with the experimental results, as shown in Table 3. The relative error between the numerical results obtained using the two plasticity theories and the experimental ultimate strength is provided between parentheses. For compact columns, the bifurcation stress and the ultimate strength are very close. In this case, the numerical predictions using the flow σ_{cr}^{FT} and the deformation theory σ_{cr}^{DT} agree well with the experimental results. Nevertheless, the slender column exhibits a large difference between the critical bifurcation point and the ultimate strength (limit point in the numerical results). The estimated limit point closely aligns with the experimental ultimate strength for both theories of plasticity.

Table 3. Numerical and experimental results.

Series	Temper	Nonlinear FE		Experiments	
		$\sigma_{cr}^{FT}\,(MPa)$	$\sigma_{cr}^{DT}\,(MPa)$	$\sigma_{cr}^{Exp}\,(MPa)$	$\sigma_{u}^{Exp}\,(MPa)$
S1	T4	133.60 (**7.74%**)	127.72 (**3%**)	124	124
	T6	248.17 (**7.4%**)	239.69 (**10.56%**)	218	268
S2	T4	79.70 (**17.21%**)	76.18 (**12.03%**)	40	68
	T6	137.82 (**12.97%**)	135.64 (**11.18%**)	38	122

In order to gain further insight into the column instability problem and the effect of geometric and material parameters, we have plotted the stress evolution against axial displacement for slenderness ratios 10.5 and 30.5 in Fig. 3 and 4, respectively. It can be seen that although the deformation theory predicts lower critical stresses than the flow theory, both theories display approximately the same trends of the stress evolution. The deformed columns inserted in these figures display the distribution of the equivalent plastic deformation PEEQ.

For low slenderness ratio $b/t = 10.5$ (Fig. 3), it can be seen from inserts that the column remains straight and elastic until the limit point, which coincides with the critical point in the experimental test. At this point, buckling occurs and the column undergoes plastic deformation. This observation aligns well with the results of (Hopperstad et al., 1999).

When the slenderness ratio takes higher value ($b/t = 30.5$), the limit point is significantly higher than the critical stress. Looking at the deformed shape, it is relevant to note that the column buckles elastically before the limit point, indicating that this point is attained in the post-buckling stage. For temper T6 with low strain hardening, the column undergoes more deformation than temper T4 prior to the limit point, which explains the great difference between the critical and the limit point (or the ultimate strength). This is in good agreement with results in literature (Hopperstad et al., 1999). Comparing the deformed shapes of the column at the limit point with the experimental test, it is clear that the nonlinear FE model predicts the same post-buckling shape.

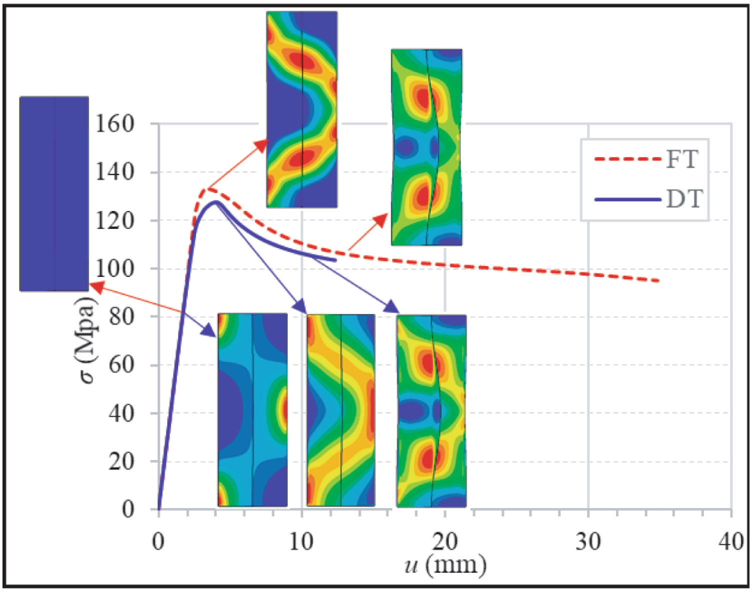

(a)

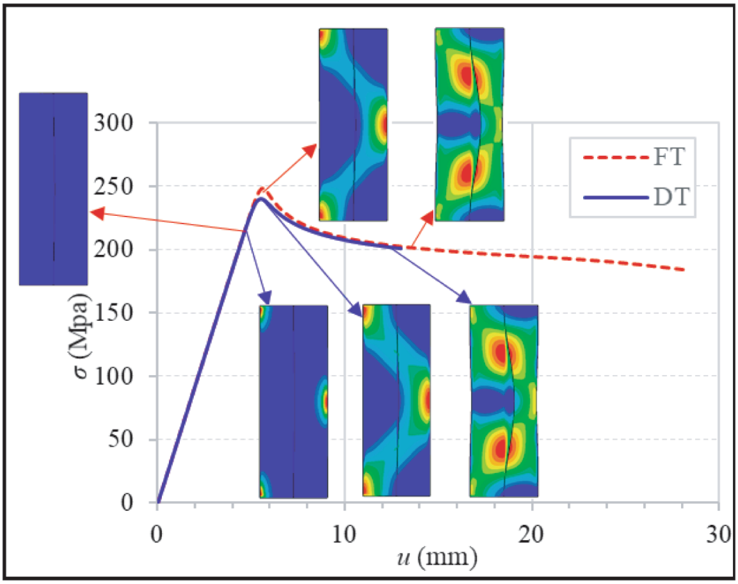

(b)

Fig. 3. Stress vs. axial displacement with flow and deformation theories (a) $b/t = 10.5$ & T4 (b) $b/t = 10.5$ & T6.

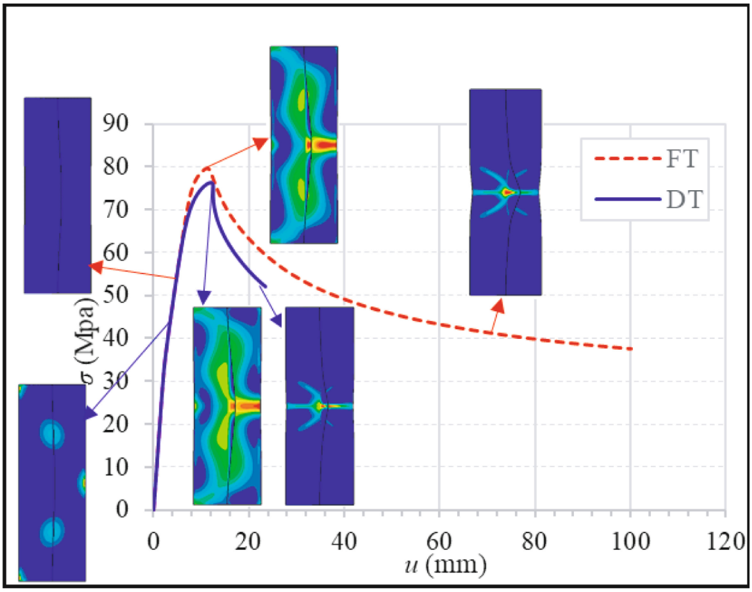

(a)

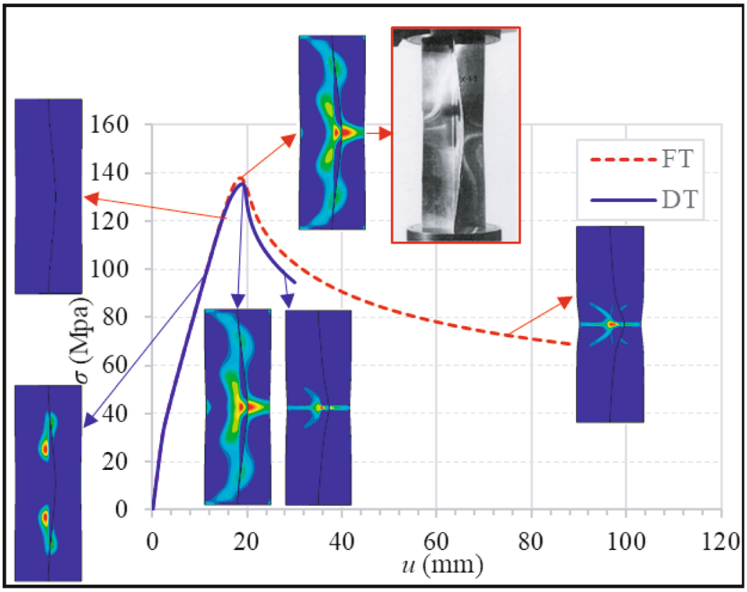

(b)

Fig. 4. Stress vs. axial displacement with flow and deformation theories (a) b/t = 30.5 & T4 (b) b/t = 30.5 & T6.

4 Conclusion

In the present study, a nonlinear FE analysis of the inelastic buckling behavior of cruciform columns was carried out using the flow and deformation plasticity theories. Columns were considered imperfect by introducing geometric initial imperfection. The effects of the column geometry and material characteristics are studied by simulating different slenderness ratios (b/t) and different strain-hardening parameters. As the Riks method is used assuming a geometric imperfection, the flow and deformation theories provide comparable results. By comparing the numerical predictions to experimental results taken from the literature, good agreement was observed. Results reveal that the difference between critical bifurcation point and limit point increases for slender column with low strain hardening material. In this case the column buckles elastically. When the columns buckle in the plastic range, the limit point (ultimate strength) coincides with the critical bifurcation point mainly for high strain-hardening material.

References

Behzadi-Sofiani, B., Gardner, L., Wadee, M.A.: Behaviour, finite element modelling and design of cruciform section steel columns. Thin-Walled Struct. (182), 110124 (2023)

Engesser, F.: Uber die Knickfestigkeit geradu strabe. Z.Architekten-Ingenieur-Vereins zu Hannover (35), 455– 462 (1889)

Gerard, G.: Introduction to Structural Stability Theory. McGraw-Hill, New York (1962)

Gerard, G., Becker, H.: Handbook of Structural Stability Part 1: Buckling of Flat Plates. NACA (1957)

Guarracino, F., Simonelli, M.: The torsional instability of a cruciform column in the plastic range: analysis of an old conundrum. Thin-Walled Struct. **113**, 273–286 (2017)

Hopperstad, O.S., Langseth, M., Tryland, T.: Ultimate strength of aluminium alloy outstands in compression: experiments and simplified analysis. Thin-Walled Struct. **34**, 279–294 (1999)

Hutchinson, J.W.: Plastic buckling. Adv. Appl. Mech. **14**, 67–144 (1974)

Hutchinson, J.W., Budiansky, B.: Analytical and numerical study of the effects of initial imperfections on the inelastic buckling of a cruciform column. In: Budiansky, B. (eds.) Buckling of Structures, pp. 98–105, LNCS. International Union of Theoretical and Applied Mechanics. Springer, Berlin, Heidelberg (1976). https://doi.org/10.1007/978-3-642-50992-6_10

Köllnera, A., Gardnerb, L., Wadee, M.A.: A new approach to the stability design of Ramberg-Osgood material struts. Structures (56), 104844 (2023)

Ramberg, W., Osgood, W.R.: Description of stress-strain curves by three parameters (902). Washington, D.C. USA (1943)

Shamass, R., Alfano, G., Guarracino, F.: A numerical investigation into the plastic buckling paradox for circular cylindrical shells under axial compression. Eng. Struct. **75**, 429–447 (2014)

Shamass, R., Alfano, G., Guarracino, F.: An investigation into the plastic buckling paradox for circularcylindrical shells under non-proportional loading. Thin-Walled Struct. **95**, 347–362 (2015)

Zhoua, W., Shia, Z., Lib, Y., Ronga, Q., Zeng, Y., Lin, J.: Elastic-plastic buckling analysis of stiffened panel subjected to global bending in forming process. Aerosp. Sci. Technol. (115), 106781 (2021)